On the Three-Directional Ray Cacti

Hiroki Katsumata[1] Satoshi Tayu[1]

Abstract: A connected graph is called a *cactus* if any two cycles have at most one vertex in common. A cactus is called a *pseudotree* if it contains at most one cycle. In this paper, We show that the characterization of 3-directional orthogonal ray cacti and 3-directional orthogonal ray pseudotrees. We also show that the recognition of 3-directional orthogonal ray cacti can be solved in polynomial time.

1. Introduction

A bipartite graph G with a bipartition (X, Y) is called an *ORG* (*orthogonal ray graph*) if there exist a family of non-intersecting rays (half-lines) R_u $(u \in X)$, parallel to the x-axis in the xy-plane, and a family of non-intersecting rays R_v $(v \in Y)$, parallel to the y-axis such that for any $u \in X$ and $v \in Y$, $(u, v) \in E(G)$ if and only if R_u and R_v intersect. An ORG is called a *3DORG* (*3-directional orhtogonal ray graph*) if every vertical ray has the same direction, or every holizontal ray has the same direction. An ORG is called a *2DORG* (*2-directional orhtogonal ray graph*) if every vertical ray has the same direction, and every holizontal ray also has the same direction. By definition, any 2DORG is a 3DORG, and any 3DORG is an ORG.

A mapping of a sum-of-product onto nano-programable logic array (nano-PLA) is inivestigated in the literature [1], [4], [8]. Since a nano-PLA can be represented by ORG and/or 3DORG [5], finding characterizations of such graphs is very important, and some problems are investigated for these graphs [3], [5], [7], [9].

A *cactus* is a connected graph in which any two cycles have at most one vertex in common. A *pseudotree* is a connected graph containing at most one cycle. A tree is a pseudotree, and pseudotree is a cactus by defintion.

An *edge-asteroid* is a sequence of edges $(e_0, e_1, \ldots, e_{2k})$ such that for each $0 \le i \le 2k$, there exists a path containing e_i and $e_{i+1 \pmod{2k+1}}$ that avoids the neighbors of the end-vertex of $e_{k+i+1 \pmod{2k+1}}$. An *A5E* (*asteroid quintuple of edges*) is a sequence of five edges $(e_0, e_1, e_2, e_3, e_4)$ such that for any $0 \le i \le 4$, there exists a path from e_i to $e_{i+1 \pmod 5}$ that avoids the neighbors of the end-vertices of $e_{i-1 \pmod 5}$ and $e_{i+2 \pmod 5}$.

Let $\mathcal{F}_1 = \{T_0, T_1, T_2, T_3\}$ be the set of four trees shown in Fig.1. The following characterizations can be found in the literature [2], [6].

Theorem I A bipartite graph G is a 2DORG if and only if it contains no edge-asteroid and no induced cycle of length at least 6. ■

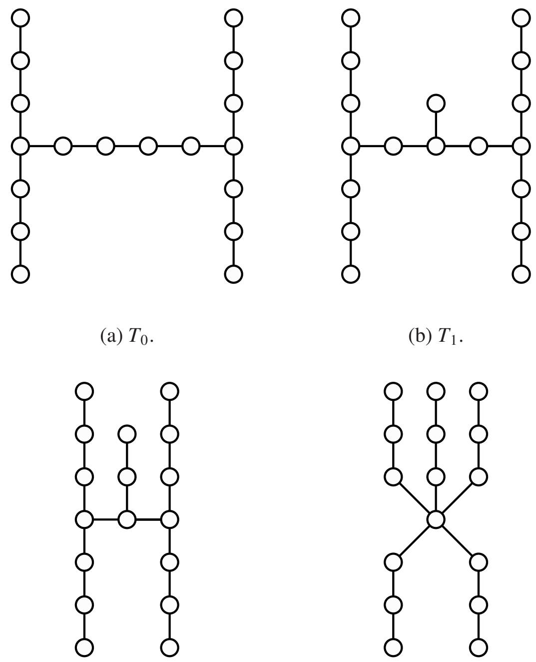

(a) T_0. (b) T_1. (b) T_2. (d) T_3.

Fig. 1 Trees in $\mathcal{F}_1$.

Theorem II The following statements are equivalent for a tree T;

(1) T is a 2DORG;
(2) T is a 3DORG;
(3) T contains no edge-asteroid;
(4) T contains no 3-claw shown in Fig.2(a) as a subtree. ■

Theorem III The following statementes are equivarent for a tree T:

- T is an ORG;
- T contains no A5E;
- T contains no tree in $\mathcal{F}_1$ as a minor. ■

Let $\mathcal{F}_2$ be the set of graphs shown in Fig.2. For any integer

1 Tokyo Institute of Technology, 2-12-1, Ookayama, Meguro, Tokyo 152–8550, Japan

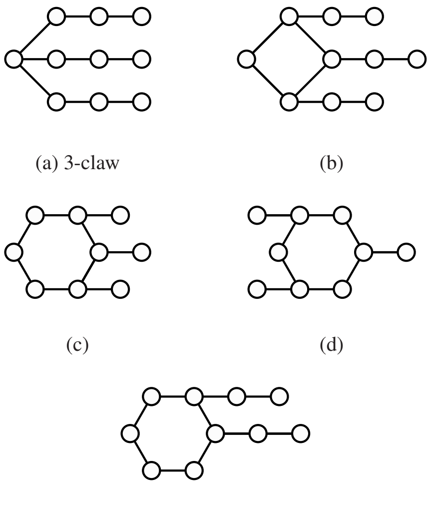

(a) 3-claw (b) (c) (d) (e)

Fig. 2 Set $\mathcal{F}_2$ of forbidden induced subgraphs.

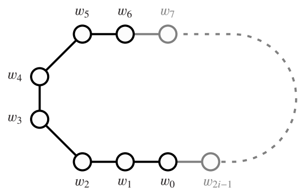

Fig. 3 Cycles in C_{2x4}.

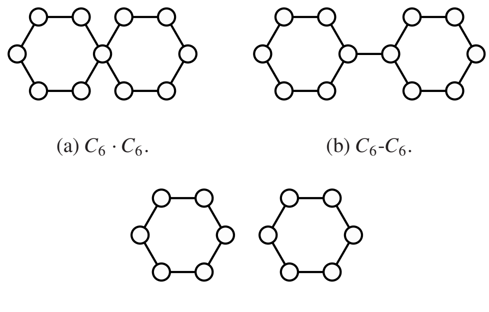

(a) $C_6 \cdot C_6$. (b) C_6-C_6. (c) $2 \times C_6$.

Fig. 4 Set $\mathcal{F}_3$ of forbidden induced subgraphs.

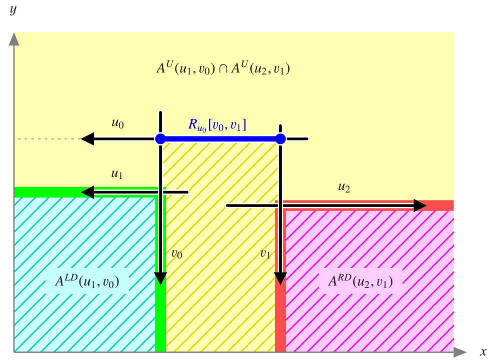

Fig. 5 Example of a Ray Representation.

$n \geq 2$, let C_{2n} be the cycle of length $2n$, and $C_{2\times n} = \{C_{2i} \mid i \geq n\}$. $C_{2\times 4}$ is the set of cycles shown in Fig. 9 for $i \geq 4$. Let $C_6 \cdot C_6$, C_6-C_6, and $2 \times C_6$ be the graphs shown in Fig.4(a), (b), and (c), respectively. The characterization of ORG and 3DORG has been open.

We show in this paper the following, where Theorem 1 is obtained as a corollary of Theorem 2.

Theorem 1 The following statements are equivalent for a bipartite pseudotree G:
(1) G is a 3DORG;
(2) G contains no edge-asteroid;
(3) G contains no graph in $C_{2\times 4} \cup \mathcal{F}_2$ as an induced subgraph. ■

Theorem 2 The following statements are equivalent for a bipartite cacti G:
(1) G is a 3DORG;
(2) G contains no edge-asteroid and no pair of cycles of length 6;
(3) G contains no graph in $C_{2\times 4} \cup \mathcal{F}_2 \cup \mathcal{F}_3$ as an induced subgraph. ■

Theorem 3 The recognition of 3-directional orthogonal ray cacti is solved in polynomial time. ■

2. Preliminaries

2.1 Ray Representation of Graphs

In this section, we assume that G is a connected 3-directional orthogonal ray graph, with diameter at least 5. We assume without loss of generality that rays of a 3DORG G parallel to y-axis are downward direction. For a vertex v of G, we denote by $(x(v), y(v))$ the coordinate of the end point of R_v. For an edge $e = (u, v)$ of G, let R_u and R_v be the rays corresponding to u and v, respectively, and $\rho(e) = (x(e), y(e))$ be the cross point of R_u and R_v. We denote by the sequence $\langle w_1, w_2, \ldots, w_p\rangle$ of the vertices the path with the vertex set $\{w_1, w_2, \ldots, w_p\}$ and edge set $\{(w_i, w_{i+1}) \mid 1 \leq i \leq p-1\}$. Let $V_D(G)$ be the set of vertices corresponding to downward rays, and $V_H(G) = V(G) - V_D(G)$. Define that

$$\begin{aligned} x_{\min} &= \min\{x(v) \mid v \in V_D(G)\}, \\ x_{\max} &= \max\{x(v) \mid v \in V_D(G)\}, \\ y_{\min} &= \min\{y(v) \mid u \in V_H(G)\}, \text{ and} \\ y_{\max} &= \max\{y(v) \mid u \in V_H(G)\}. \end{aligned}$$

For $(w, w') \in E(G)$, let $R_w[w']$ be a partial ray of R_w whose end point is just the cross point of R_w and $R_{w'}$. Since R_w and $R_{w'}$ intersect, R_w and $R_{w'}$ divide the plane into two areas say $A^D(w, w')$ and $A^U(w, w')$, where $A^U(w, w')$ is the area containing $\{(x, y) \mid y \geq y_{\max}\}$.

For any vertex $w \in V(G)$ and its adjacent vertices w', w'' in G, let $R_w[w', w'']$ be a line segment with endpoints $\rho((w, w'))$ and $\rho((w, w''))$. For an induced path $P = \langle w_0, w_1, \ldots, w_p\rangle$ of G, let

$$B[P] = R_{w_0}[w_1] \cup R_{w_p}[w_{p-1}] \cup \bigcup_{i=2}^{p-1} R_{w_i}[w_{i-1}, w_{i+1}].$$

The upper and lower sides of $B[P]$ are denoted by $A^U[P]$ and $A^D[P]$, respectively.

As an example, we show in Figure 5 a ray representation of a path $P = \langle u_1, v_0, u_0, v_1, u_2\rangle$, such that R_{u_0} and R_{u_1} are leftward rays with $x_{u_0} < x_{u_1}$, R_{v_0} and R_{v_1} are downward rays with $x_{v_0} < x_{v_1}$, and R_{u_2} is a rightward ray, where (x_v, y_v) is the endpoint of the ray R_v corresponding to v. Green rays are $R_{v_0}[u_1]$ and $R_{u_1}[v_0]$ dividing the plane into two areas $A^D(u_1, v_0)$ and $A^U(u_1, v_0)$, and red rays are $R_{v_1}[u_2]$ and $R_{u_2}[v_1]$ dividing into $A^D(u_2, v_1)$ and $A^U(u_2, v_1)$. A blue line segment shows $R_{u_0}[v_0, v_1]$. $A^D[\langle u_1, v_0, u_1, v_1, u_2\rangle]$ is the area shown by diagonal lines.

By definition, we have the following.

Lemma 1 Let $P = \langle w_0, w_1, \ldots, w_p\rangle$ be an induced subpath of a 3DORG. Then, xy-plane is separated by $B[P]$ into two regions ■

For an edge (u, v) of a 3DORG G with $u \in X$, Let

$$A^{LD}(u, v) = \{(x, y) \mid x < x(v), y < y(u)\}, \text{ and}$$
$$A^{RD}(u, v) = \{(x, y) \mid x > x(v)\} \cup \{(x, y) \mid y > y(u)\}.$$

It should be noted that $B[\langle u, v\rangle]$ separates the xy-plane.

For a graph G and vertices $u, v \in V(G)$, let $\mathrm{dist}_G(u, v)$ be the distance between u and v in G. For a subgraph S of G and $w \in V(G)$, let $\mathrm{dist}_G(S, w) = \min_{u\in V(S)} \mathrm{dist}_G(u, w)$. An induced subpath of G is called an *edge-spine* of G if at least one endvertex of any edge of G is within distance one from at least one vertex of the path.

Lemma 2 Let $\mathcal{R}(G)$ be a 3-directional orthogonal ray representation of G, and let u_L and u_R be the vertices corresponding the leftward and rightward rays of minimum y-coordinates, respectively. Then, an induced u_L-u_R path P of G is an edge-spine.

Proof. We assume without loss of generality that $\mathcal{R}(G)$ is not a 2-directional orthogonal ray representation.

Let v_L $[v_R]$ be the adjacent vertex of u_L $[u_R]$, in P. It suffices to show that for any edge (u, v),

$$\mathrm{dist}_G(P, u) \le 1 \text{ or} \quad (1)$$
$$\mathrm{dist}_G(P, v) \le 1. \quad (2)$$

Case 1: u is a leftward ray.
If u or v is in P, (1) or (2) holds. So, we assume that that u and v are outside P. If a vertex $w \in V(P)$ has a downward ray R_w with $x(w) < x(v_L)$, R_w and R_{u_L} intersect, and this contradicts to P to be an induced path. Therefoer,

$$\{(x, y) \mid x < x(v_L), y > y(u_L)\} \cap B[P] = \emptyset, \text{ i.e.,}$$
$$\{(x, y) \mid x < x(v_L), y > y(u_L)\} \subset A^U[P].$$

Since u is leftward and $y(u) > y(u_L)$, a partial ray $\{(x, y(u)) \mid x < x(v_L)\}$ of R_u is contained in $A^U[P]$. Therefore, we have

$$A^U[P] \cap R_u \neq \emptyset. \quad (3)$$

Since R_v is downward,

$$\{(x(v), y) \mid y < y_{\min}\} \subset R_v,$$

and we have

$$A^D[P] \cap R_v \neq \emptyset. \quad (4)$$

From Lemma 1, (3), and (4), we have that $R_u \cup R_v$ intersect $B[P]$, i.e., R_u or R_v intersects $B[P]$.

Thus, we have (1) or (2).

Case 2: u is a rightward ray.
By the similar arguments to the proof of Case 1, we have the lemma. ■

As a corollary of Lemma 2, we have the following.

Corollary 1 A connected 3DORG has an edge-spine as an induced subgraph. ■

It should be noted that there is connected bipartite graph containing an edge-spine as an induced subgraph, but not a 3DORG.

2.2 3-Directional Orthogonal Ray Graph with an Induced Subcycle of Length 6

In this subsection, we consisder a ray representation of a 3DORG G containing C_6 as an induced subgraph. For a positive integer i, we denote that $[i] = \{0, 1, \ldots, i\}$. Define that

$$V(C_6) = \{w_i \mid i \in [5]\}, \text{ and}$$
$$E(C_6) = \{(w_i, w_{i+1 (\mathrm{mod}\ 6)}) \mid i \in [5]\}.$$

Consider any ray representation $\mathcal{R}(G)$ of G. For any $i \in [5]$, let R_i be the ray of $\mathcal{R}(G)$ corresponding to w_i, and (x_i, y_i) be the xy-coordinate of the end point of R_i. We assume without loss of generality that R_0, R_2, R_4 are vertical, and R_2 and R_4 are the left and right most vertical rays, respectively, i.e., $x_2 < x_0 < x_4$.

We now see that

$$y_1, y_5 \le y_0 < y_3 \le y_2, y_4 \quad (5)$$

Since R_3 intersects both R_2 and R_4, we have $y_2, y_4 \ge y_3$,

$$\{(x, y_3) \mid x_2 \le x_4\} \subset R_3 \text{ and} \quad (6)$$
$$(x_0, y_3) \in R_3. \quad (7)$$

Since R_0 and R_3 does not intersect,

$$(x_0, y_3) \notin R_0 = \{(x_0, y) \mid y \le y_0\}$$

by (7). Therefore, we have $y_3 > y_0$. Since R_1 and R_5 intersect R_0, $y_1, y_5 < y_0$. Thus, we have (5).

We next see that

$$x_2 < x_5 \le x_0 \le x_1 < x_4, \quad (8)$$

and that R_1 and R_5 are leftward and rightward rays, respectively. Since R_1 intersects both R_0 and R_2,

$$\{(x, y_1) \mid x_2 \le x \le x_0\} \subset R_1. \quad (9)$$

From $x_0 < x_4$ and $y_1 < y_4$, R_1 is leftward and $x_1 < x_4$, since R_1 does not intersect R_4. Thus from (9), $x_0 \le x_1$. Similarly, we also have $x_2 < x_5 \le x_0$ and R_5 to be rightward.

Let $Y^L_{\min}(C_6)$ and $Y^R_{\min}(C_6)$ be the minimum y-coordinates of leftward and rightward rays corresponding to a vertex of C_6, respectively. Similarly, let $X_{\min}(C_6)$ and $X_{\max}(C_6)$ be the minimum and maximum x-coordinates of downward rays corresponding to a vertex of C_6, respectively. Let

$$A^{LD}(C_6) = \{(x, y) \mid x < X_{\min}, y < Y^L_{\min}(C_6)\} \text{ and}$$
$$A^{RD}(C_6) = \{(x, y) \mid x > X_{\max}, y < Y^R_{\min}(C_6)\}.$$

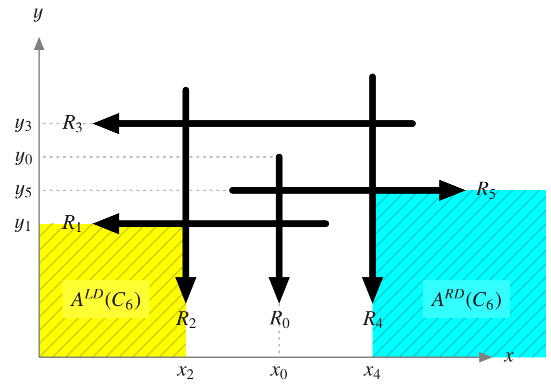

Fig. 6 Ray Representation of C_6.

Figure 6 shows an example of a ray representation of C_6 in case that R_3 is leftward, and $y_1 < y_5$. Since R_3 intersects both R_2 and R_4, if R_3 is leftward, then $x_3 \geq x_4$ and otherwise, $x_3 \leq x_2$. $A^{LD}(C_6)$ and $A^{RD}(C_6)$ are shown by yellow and cyan areas, respectively.

A connected graph H with a subgraph S is said to be *edge-separable* by S if all vertices in $V(S)$ belong to different connected components in $H - E(S)$. For any $v \in V(S)$ and the connected component C of $H - E(S)$ containing v, we denote by

$$\mathrm{depth}^H_S(v) = \max_{w \in V(C)} \mathrm{dist}_C(v, c).$$

By definition, we have the following.

Lemma 3 A connected graph H is a cactus if and only if it is edge-separable by any induced subcycle. ■

Lemma 4 If G is edge-separable by C_6 then $\mathrm{depth}^G_{C_6}(v_0) = \mathrm{depth}^G_{C_6}(v_3) = 0$.

Proof. If v_0 is adjacent with a vertex u outside C_6, then R_u is holizontal. Let P be the path induced by $\{v_2, v_3, v_4\}$. It should be noted that the cross point (x_0, y_u) of R_0 and R_u is inside $A^D[P]$. If R_u is rightward ray, $\{(x, y_u) \mid x > x_0\} \subset R_u$. Therefore, R_u intersects R_4, since $x_0 < x_4$ and $y_u < y_4$. This implies that u is also adjacent with v_4. Thus, G is not edge-separable by C_6. Similarly, if R_u is leftward ray, G is not edge-separable.

Therefore, v_0 is not adjacent with any vertex outside C_6, and $\mathrm{depth}^G_{C_6}(v_0) = 0$.

If v_3 is adjacent with a vertex u outside C_6, then R_u is a downward ray containing (x_u, y_3), the cross point of R_u and R_3. Let $P = \langle v_1, v_0, v_5 \rangle$. Since $(x_u, y_3) \in A^U[P]$ and R_u is a downward ray, R_u intersects $B[P]$. Therefore, G is not edge-separable.

Therefore, v_3 is not adjacent with any vertex outside C_6, and $\mathrm{depth}^G_{C_6}(v_0) = 0$.

Thus, we have the lemma. ■

For $i \in [5]$, let Γ_i be the connected component of $G - E(C_6)$ containing v_i.

Lemma 5 If G is edge-separable by C_6, and Γ_i contains a vertex w independent from C_6 with $\mathrm{dist}_G(w, v_i) = 2$ for some $i \in \{1, 2\}$, then there exists a vertex $z \in V(\Gamma_i)$ adjacent with both v_i and w in Γ_i such that $R_z \cap A^{LD}(C_6) \neq \emptyset$.

Proof. Consider in case of $i = 1$. The lemma can be proved similarly when $i = 2$.

Let z be a vertex adjacent with both w and v_1, and we show the lemma by contradiction. Suppose that

$$R_z \cap A^{LD}(C_6) = \emptyset. \tag{10}$$

From $(z, v_1) \in E(C_6)$ and (10), $x_2 < x(z) \leq x_1$, since R_z is vertical. Thus from (6) and (10), $y(z) < y_3 \leq y_2$. Therefore, R_z intersects R_2, and we have contradiction. Thus, $R_z \cap A^{LD}(C_6) = \emptyset$, and we have the lemma. ■

Lemma 6 If G is edge-separable by C_6, then $\mathrm{depth}^G_{C_6}(v_1) \leq 1$ or $\mathrm{depth}^G_{C_6}(v_2) \leq 1$.

Proof. Assume contrary that $\mathrm{depth}^G_{C_6}(v_1) \geq 2$ and $\mathrm{depth}^G_{C_6}(v_2) \geq 2$. From Lemma 5, Γ_1 and Γ_2 contain vertices z_1 and z_2 such that

$$R_{z_1} \cap A^{LD}(C_6) \neq \emptyset \text{ and}$$
$$R_{z_2} \cap A^{LD}(C_6) \neq \emptyset,$$

respectively. Since R_{z_1} is vertical and $(z_1, v_1) \in E(\Gamma_1)$, we have

$$\{(x(z_1), y) \mid y \leq y_1\} \subseteq R_{z_1}.$$

Similarly, we also have

$$\{(x, y(z_2)) \mid x \leq x_2\} \subseteq R_{z_2}.$$

Therefore, R_{z_1} and R_{z_2} intersect, and we have contradiction. Thus, $\mathrm{depth}^G_{C_6}(v_1) \leq 1$ or $\mathrm{depth}^G_{C_6}(v_2) \leq 1$, and we have the lemma. ■

By similar arguments to the proof of Lemma 6, we also have the following.

Lemma 7 If G is edge-separable by C_6, then $\mathrm{depth}^G_{C_6}(v_4) \leq 1$ or $\mathrm{depth}^G_{C_6}(v_5) \leq 1$. ■

Lemmas 4, 6, and 7, we have the following.

Corollary 2 If G is edge-separable by C_6, $\mathrm{depth}^G_{C_6}(v_0) = \mathrm{depth}^G_{C_6}(v_3) = 0$, $\min(\mathrm{depth}^G_{C_6}(v_1), \mathrm{depth}^G_{C_6}(v_2)) \leq 1$, and $\min(\mathrm{depth}^G_{C_6}(v_4), \mathrm{depth}^G_{C_6}(v_5)) \leq 1$. ■

A sequence of such depths of a subcycle C is called a *depth-sequence* of C. It should be noted that the following depth-sequences are equivalent; $(1, 2, 3, 4, 5, 6)$, $(6, 1, 2, 3, 4, 5)$, $(6, 5, 4, 3, 2, 1)$, and so on. We use $\mathrm{depth}^G_C(v) = 2^+$ instead of $\mathrm{depth}^G_C(v) = l$ for any integer $l \geq 2$, and $\mathrm{depth}^G_C(v) = 1^-$ instead of $\mathrm{depth}^G_C(v) = 0$ or 1. We also use $*$ as a wild card in the depth sequence. Corollary2, we have the following.

Lemma 8 If a 3DORG has an induced cycle C_6 of length 6 then the depth sequcen of C_6 is $(0, 1^-, *, 0, 1^-, *)$ or $(0, 1^-, *, 0, *, 1^-)$. ■

In particular, if C_6 has two vertex with depth at least 2, then the depth sequcen of C_6 is $(0, 1^-, 2^+, 0, 1^-, 2^+)$ or $(0, 1^-, 2^+, 0, 2^+, 1^-)$.

2.3 Edge-Spine and Edge-Asteroid

An induced cycle of length 6 is said to be *feasible* if its depth sequence forms $(0, *, *, 0, *, *)$.

Lemma 9 If a bipartite cactus G has an edge-spine P and any induced cycle of length 6 is feasible, then G has no edge-asteroid.

Proof. We show the lemma by contradiction.

Suppose that G has a lngest edge-spine $P = \langle v_0, v_1, \ldots, v_p \rangle$ and an edge-asteroid $(e_0, e_1, \ldots, e_{2k})$.

For $i \in [2k]$, we define $J(e_i)$ is the minimum integer j such that v_j adjacent with one endvertex of e_i.

Without loss of generality that $J(e_0) \leq J(e_i)$ for any $i \in [2k]$.

We denote by $e_k \prec e_l$ if one of the following holds
- $J(e_k) < J(e_l)$, or
- $J(e_k) = J(e_l) = j$ and there exist a path connecting e_k and v_{j-1} avoinding v_j.

Since G is a bipartite cactus, $e_k \not\prec e_l$ if $e_k \prec e_l$.

Then, we can prove the following two propositions.

Proposition 1 If $e_i \prec e_{i+k+1 (\mathrm{mod}\ 2k+1)}$, then $e_{i+1 (\mathrm{mod}\ 2k+1)} \prec e_{i+k+1 (\mathrm{mod}\ 2k+1)}$. ■

Proposition 2 If $e_i \prec e_{i+k (\mathrm{mod}\ 2k+1)}$, then $e_i \prec e_{i+k+1 (\mathrm{mod}\ 2k+1)}$. ■

From these proposition, we have $e_i \prec e_{i+k (\mathrm{mod}\ 2k+1)}$ and $e_i \prec e_{i+k+1 (\mathrm{mod}\ 2k+1)}$ for any $i \in [2k]$. However, $e_0 \prec e_{k+1} \prec e_{2k+1 (\mathrm{mod}\ 2k+1)} = e_0$ and we have contradiction.

Thus, we have the lemma. ■

2.4 Forbidden Induced Subgraphs of Cactus

In this subsection, we consider a bipartite cactus G contains no graph in $C_{2\times 4} \cup \mathcal{F}_2 \cup \mathcal{F}_3$ as an induced subgraph.

Lemma 10 G contains at most one cycle of length 6 whose depth sequence is $(0, 1^-, *, 0, 1^-, *)$ or $(0, 1^-, *, 0, *, 1^-)$,

Proof. Since any graph in $\mathcal{F}_3$ is not contained as a subgraph of G, G contains at most one cycle of length 6. Since Fig.2(c) and (d) are in $\mathcal{F}_2$, whose depth sequence forms $(0, *, *, 0, *, *)$. Moreover, since Fig.2(e) is in $\mathcal{F}_2$, the depth sequence forms $(0, 1^-, *, 0, 1^-, *)$ or $(0, 1^-, *, 0, *, 1^-)$, and we have the lemma. ■

Since Fig.2(b) is in $\mathcal{F}_2$, we have the following.

Lemma 11 A depth sequence of any cycle $C \subseteq G$ of length 4 forms $(1^-, 1^-, *, *)$, or $(1^-, *, 1^-, *)$. ■

We define *anchors* for each cycle, and we will prove that G has an edge-spine containing all anchors.

For a cycle of length 6 with depth sequence $(0, 1^-, *, 0, 1^-, *)$ or $(0, 1^-, *, 0, *, 1^-)$, the vertices of C_6 corresponding to $*$ are set to be anchor. (See Lemma 10.)

For a cycle C of length 4, we set anchors as follows. (See Lemma 11.)

Case 1 the depth sequence forms $(1^-, 1^-, 1^-, 1^-)$.
arbitrary two vertices are set to be an anchor.

Case 2 the depth sequence forms $(1^-, 1^-, 1^-, 2^+)$.

Case 2-1 the depth sequence forms $(1^-, 0, 1^-, 2^+)$.
the vertex of C corresponding to 2^+ is set to be an anchor.

Case 2-2 the depth sequence forms $(1^-, 1, 1^-, 2^+)$.
the vertices of C corresponding to 2^+ and 1 are set to be anchors.

Case 3 the depth sequence forms $(1^-, 1^-, 2^+, 2^+)$ or $(1^-, 2^+, 1^-, 2^+)$.
the vertices of C corresponding to 2^+ are set to be anchors.

Let S be the minimal connected subgraph of G containing all anchors. Since G contains no 3-claw, we can prove that S is a path, and there is an edge-spine P containing S.

Lemma 12 If a bipartite cactus G does not contain 3-claw as an induced subgraph, then G contains an edge spine.

Proof. Let $P = \langle u_0, u_1, \ldots, u_d \rangle$ be a maximal induced path of G. Assume that there exists an edge $(w, w') \in E(G)$ such that $\mathrm{dist}_P(w) \geq 2$ and $\mathrm{dist}_P(w') \geq 2$. Without loss of generality we assume that $\mathrm{dist}_P(w') \geq \mathrm{dist}_P(w)$, and $\mathrm{dist}(u_i, w) = \mathrm{dist}_P(w)$. Let P' be a shortest path connecting w' and u_i containing w. Since P is maximal, $3 \leq i \leq d-3$. Since w' does not adjacent with any vertex of P, the subgraph induced by $V(P') \cup \{u_j \mid i-3 \leq j \leq i+3\}$ contains 3-claw or its subdivision, that is, G contains a 3-claw as an induced subgraph.

Thus, if G does not contain 3-claw as an induced subgraph, then G contains an edge spine. ■

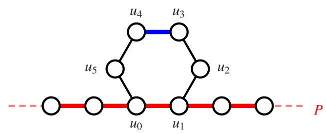

Fig. 7 $C \cup P$ in case of $V(C) \cap V(P) = \{c_0, c_1\}$.

Lemma 13 Let G be a bipartite cactus containing an edge spine P and induced cycle C of length 6. Then, $|V(C) \cap V(P)| \geq 3$

Proof. Let C be the cycle represented by

$$V(C) = \{c_i \mid i \in [5]\}, \text{ and}$$
$$E(C) = \{(c_i, c_{i+1}) \mid i \in [4]\} \cup \{(c_0, c_5)\}.$$

We show the lemma by contradiction.

Assume contrary that $|V(C) \cap V(P)| \leq 2$. If $|V(C) \cap V(P)| = 0$ or 1, the proof is rather obvious. So, we assume without loss of generality that

$$V(C) \cap V(P) = \{u_0, u_1\}.$$

Fig. 7 shows an example of C and P in case of $V(C) \cap V(P) = \{u_0, u_1\}$. Then, the endvertices of (u_3, u_4) satisfies $\mathrm{dist}_P(u_3), \mathrm{dist}_P(u_4) \geq 2$. However, this contradicts to P to be an edge-spine, and we have contradiction.

Thus, we have the lemma. ■

Lemma 14 If a bipartite cactus G has an edge-spine and G contains no induced subgraph isomorphic to Fig. 2(b), then G also has a maxmal edge-spine P such that for any induced cycle C of length 4 with $E(P) \cap E(C) = \{(u, v), (v, w)\}$, the degree of every neighbor of v outside P is 1.

Proof. Since G contains no induced subgraph isomorphic to Fig. 2(b),

$$\min\left\{\mathrm{depth}^G_C(u), \mathrm{depth}^G_C(v), \mathrm{depth}^G_C(w)\right\} \leq 1. \quad (11)$$

If $\mathrm{depth}^G_C(v) \leq 1$, we have the lemma.

Otherwise, let $\langle v, y, z \rangle$ is a subpath of G with $y, z \notin V(P)$. Since P is a maximal edge-spine, P contains $\langle t, u, v, w, x \rangle$ as a subpath such that t and x are outside P. See Fig. 8. From (11), one of t and x is a degree 1 vertex. We assume without loss of generality that $\deg_G(x) = 1$, i.e., x is the one endvertex of the edge-spine. Then, replacing w and x to y and z, respectively, we obtain a new edge-spine with $|E(P) \cap E(C)| = 1$. Thus by applying the replacement to the both ends of P, if any, we obtain a new edge-spine P' satisfying the statements of the lemma. ■

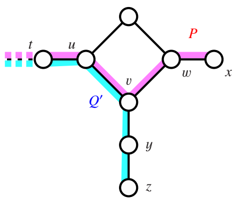

Fig. 8 around cyle C.

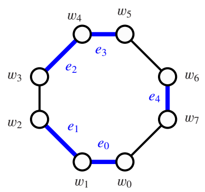

Fig. 9 cycle C of length 8.

Table 1 $V(e_i)$, $V(e_{i+1})$, and $N(e_{i+k+1})$ for the graph shown in Fig. 10(a).

i	$V(e_i)$	$V(e_{i+1 \pmod{2k+1}})$	$N(e_{i+k+1 \pmod{2k+1}})$
0	$\{w_0, w_1\}$	$\{w_1, w_5\}$	$\{w_3, w_4, w_5, w_6\}$
1	$\{w_1, w_2\}$	$\{w_3, w_5\}$	$\{w_5, w_6, w_7, w_{8 \pmod{2n}}\}$
2	$\{w_3, w_4\}$	$\{w_4, w_5\}$	$\{w_{2n-1}, w_0, w_1, w_2\}$
3	$\{w_4, w_5\}$	$\{w_6, w_5\}$	$\{w_0, w_1, w_2, w_3\}$
4	$\{w_6, w_7\}$	$\{w_0, w_5\}$	$\{w_2, w_3, w_4, w_5\}$

3. Proof Sketch of Theorem 2

From Corollary 1, Lemmas 8 and 9, we have the following.

Lemma 15 If (1) of Theorem 2 holds, then (2) also holds. ■

Lemma 16 If (2) of Theorem 2 holds, then (3) also holds.

Proof. Suppose that (3) of Theorem 2 does not hold.

Case 1: G contain an induced cycle C of length $2n$ for some $n \geq 4$.

If $n \geq 5$, the proof is rather obvious. So, we only consider in case that $n = 4$. Let

$$V(C) = \{w_0, w_1, \ldots, w_{2n-1}\} \text{ and}$$
$$E(C) = \{(w_0, w_1), (w_1, w_2), \ldots, (w_{2n-2}, w_{2n-1}), (w_{2n-1}, w_0)\}.$$

Define that $e_0 = (w_0, w_1)$, $e_1 = (w_1, w_2)$, $e_2 = (w_3, w_4)$, $e_3 = (w_4, w_5)$, and $e_4 = (w_6, w_7)$. We now see that $\{e_i \mid i \in [4]\}$ is an edge asteroid of $2k + 1 = 5$ edges in the cycle.

For an edge e, let $V(e)$ be the set of the endvertices of e, and $N(e)$ be the the set of neighbours of the endvertices of e, It should be noted that for any edge e, $V(e) \subseteq N(e)$. Let P_i be the subgraph induced by $V(e_i) \cup V(e_{i+1 \pmod 5})$. From Table. 1, it is easy to verify that $V(P_i) \cap N(e_{i+k+1 \pmod 5}) = \emptyset$, since $V(e_i) \cup V(e_{i+1 \pmod 5}) = V(P_i)$. Therefore, P_i is a path containing e_i and $e_{i+1 \pmod 5}$ that avoids the vertices in $N(e_{i+k+1 \pmod 5})$.

Thus, (2) of Theorem 2 does not hold.

Case 2: G contains an induced subgraph S isomorphic to one graphs in Fig. 2.

Case 2-1: S is isomorphic to 3-claw shown in Fig. 2(a).

We will show that S contains an edge-asteroid (e_0, e_1, e_3) shown in Fig. 10(a). It should be noted that $N(e_i) = V(e_i) \cup \{w_i\}$. For any $i \in [2]$, let P_i be the subgraph induced by $N(e_i) \cup$

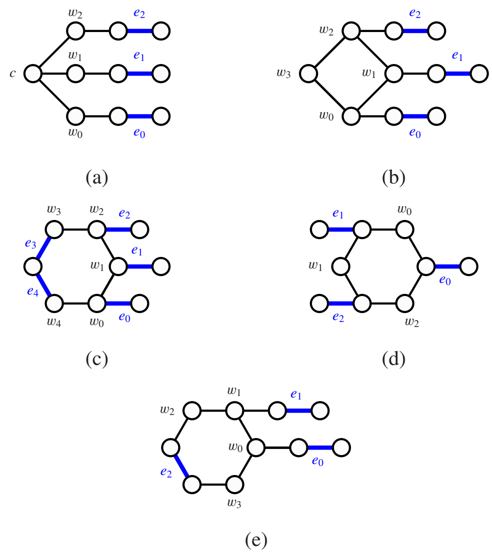

Fig. 10 Edge-asderoids for forbidden induced subgraphs

$N(e_{i+1 \pmod 3}) \cup \{c\}$. Then,

$$V(P_i) \cap N(e_{i+2 \pmod 3})$$
$$= (N(e_i) \cup N(e_{i+1 \pmod 3}) \cup \{c\}) \cap N(e_{i+2 \pmod 3})$$
$$= \emptyset$$

Since $e_i, e_{i+1 \pmod 3} \in E(P_i)$, P_i is a path containing e_i and $e_{i+1 \pmod 3}$ that avoids the vertices in $N(e_{i+2 \pmod 3})$.

Thus, (2) of Theorem 2 does not hold.

Case 2-2: S is isomorphic to the graph shown in Fig. 2(b).

We will show that S contains an edge-asteroid (e_0, e_1, e_3) as shown in Fig. 10(b). $N(e_i) = V(e_i) \cup \{w_i\}$. For $i = 0, 1$, let P_i be the subgraph induced by $N(e_i) \cup N(e_{i+1 \pmod 3})$, and P_2 be the subgraph induced by $N(e_2) \cup N(e_0) \cup \{w_3\}$. For $i = 0, 1$,

$$V(P_i) \cap N(e_{i+2 \pmod 3})$$
$$= (N(e_i) \cup N(e_{i+1 \pmod 3})) \cap N(e_{i+2 \pmod 3})$$
$$= \emptyset, \text{ and}$$
$$V(P_2) \cap N(e_1)$$
$$= (N(e_0) \cup N(e_2 \cup \{w_3\})) \cap N(e_1)$$
$$= \emptyset.$$

Since $e_i, e_{i+1 \pmod 3} \in E(P_i)$, P_i is a subgraph containing e_i and $e_{i+1 \pmod 3}$ that avoids the vertices in $N(e_{i+2 \pmod 3})$.

Thus, (2) of Theorem 2 does not hold.

Case 2-3: S is isomorphic to the graph shown in Fig. 2(c).

In this case, we will show that S contains an edge-asteroid $(e_0, e_1, e_3, e_4, e_5)$ shown in Fig. 10(c). It should be noted that

$$w_i \in V(e_i) \quad \forall i \in [4], \tag{12}$$
$$N(e_i) = V(e_i) \cup \{w_{i-1 \pmod 5}, w_{i+1 \pmod 5}\} \quad \forall i \in [4], \tag{13}$$
$$w_i \notin V(e_j) \quad \forall i, j \in [4] \text{ with } i \neq j, \text{ and} \tag{14}$$
$$V(e_i) \cap V(e_j) = \emptyset \quad \forall i, j \in [4] \text{ with } |i - j| \in \{2, 3\}. \tag{15}$$

Let P_i be the subgraph induced by $V(e_i) \cup V(e_{i+1 \pmod 5})$. From (12)–(15),

$$\begin{aligned} &V(P_i) \cap N(e_{i+3 \pmod 5}) \\ &= (V(e_i) \cup N(e_{i+1 \pmod 5})) \cap N(e_{i+3 \pmod 5}) \\ &= \emptyset \end{aligned}$$

for any $i \in [4]$.

Since $e_i, e_{i+1 \pmod 5} \in E(P_i)$ for each $i \in [4]$, P_i is a path containing e_i and $e_{i+1 \pmod 5}$ that avoids the vertices in $N(e_{i+3 \pmod 5})$.

Thus, (2) of Theorem 2 does not hold.

Case 2-4: S is isomorphic to the graph shown in Fig. 2(d).

In this case, we will show that S contains an edge-asteroid (e_0, e_1, e_3) shown in Fig. 10(d). It should be noted that

$$N(e_i) = V(e_i) \cup \{w_i, w_{i-1 \pmod 3}\} \quad \forall i \in [2]. \tag{16}$$

For $i \in [2]$, let P_i be the subgraph induced by $V(e_i) \cup \{w_i\} \cup V(e_{i+1 \pmod 3})$. From (16), we have

$$\begin{aligned} &V(P_i) \cap N(e_{i+2 \pmod 3}) \\ &= (V(e_i) \cup \{w_i\} \cup V(e_{i+1 \pmod 3})) \\ &\quad \cap (V(e_{i+2 \pmod 3}) \cup \{w_{i+2 \pmod 3}, w_{i+1 \pmod 3}\}) \\ &= \emptyset \end{aligned}$$

for $i \in [2]$.

Since $e_i, e_{i+1 \pmod 3} \in E(P_i)$, P_i is a path containing e_i and $e_{i+1 \pmod 3}$ that avoids the vertices in $N(e_{i+2 \pmod 3})$.

Thus, (2) of Theorem 2 does not hold.

Case 2-5: S is isomorphic to the graph shown in Fig. 2(e).

In this case, we will show that S contains an edge-asteroid (e_0, e_1, e_3) shown in Fig. 10(e). It shouid be noted that for $i = 0, 1$, $N(e_i) = V(e_i) \cup \{w_i\}$, and $N(e_2) = V(e_2) \cup \{w_2, w_3\}$. Therefore,

$$N(e_i) \cap N(e_j) = \emptyset \qquad \forall i \in [2]. \tag{17}$$

For $i \in [2]$, let P_i be the subgraph induced by $N(e_i) \cup N(e_{i+1 \pmod 3})$. From (17),

$$\begin{aligned} &V(P_i) \cap N(e_{i+2 \pmod 3}) \\ &= (N(e_i) \cup N(e_{i+1 \pmod 3}) \cap N(e_{i+2 \pmod 3}) \\ &= \emptyset \quad \forall i \in [2]. \end{aligned}$$

Since $e_i, e_{i+1 \pmod 3} \in E(P_i)$, P_i is a path containing e_i and $e_{i+1 \pmod 3}$ that avoids the vertices in $N(e_{i+2 \pmod 3})$.

Thus, (2) of Theorem 2 does not hold.

Case 3: G contains an induced subgraph S isomorphic to one of graphs in Fig. 4.

Since G contains two induced cycles of length 6, (2) of Theorem 2 does not holds.

Thus, we have the lemma. ■

Lemma 17 If (3) of Theorem 2 holds, then (1) also holds. ■

We will show Lemma 17 in Section 3.2. From Lemmas 15, 16, and 17, we have Theorem 2. As a corollary of Theorem 2, we also have Theorem 1. In the proof of Lemma 17 in we show the construction of ray representation of G along an edge-spine. Since such an edge-spine can be found in polynomial time, we can recognize whether G is 3DORG. Thus, we have Theorem 3.

Before proving Lemma 17, we need some preliminaries.

(a) (b)

Fig. 11 Example of red vertices.

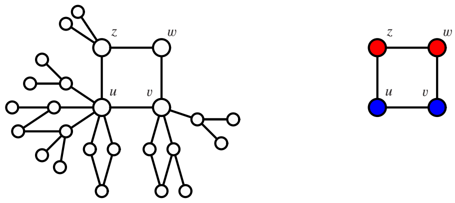

(a) (b)

Fig. 12 Example of blue vertices.

3.1 Preliminaries of Lemma 17

For a graph S and a vertex $u \in V(S)$, if a vertex u is represented by a red circle in a figure of S, the figure implies the graph obtained from S and a rooted tree of height at most 1 by identifying u and the root of the tree. Such a vertex is called a red vertex. Fig. 11(a) is an example of a graph represented by Fig. 11(b).

A graph represented by Fig. 11(b) is called a *diamond*, and the vertex r is the *root* of it.

For a graph S and a vertex $u \in V(S)$, if a vertex u is represented by a blue circle in a figure of S, the figure implies the graph obtained from S, a number of diamonds, and a rooted trees of height at most 2 by identifying u and the roots of those diamonds and trees. Such a vertex is called a blue vertex. Fig. 12(a) is an example of a graph represented by Fig. 12(b).

Rays corresponding to vertices of a diamond shown in Fig. 13(a) can be drawn in an L-shaped area and R_a as seen in Fig. 13(b), where L-shaped area is represented by blue area in the figure. Since a large L-shaped area can contain a number of small L-shaped areas, we have the followning.

Proposition 3 A blue vertex rooted at r can be drawn in an L-shaped are and R_r as seen in Fig. 13(c). ■

From Proposition 3, we also have that Fig. 12(b) can be represented by Fig. 14(a), that is, we have the following.

Proposition 4 A ray representation for Fig. 12(b) can be drawn in an L-shaped area and two rays R_u and R_v as shown in Fig. 14(b). ■

For a diamond with two blue vertices shown in Fig. 15(a), we have the following.

Proposition 5 A ray representation for Fig. 15(a) can be drawn in an L-shaped area and two rays R_u and R_w as shown in Fig. 15(b). ■

3.2 Proof of Lemma 17

In this section, we show an example of a bipartite cactus and construction of its ray representation.

From Lemmas 10, 11, 12, 13, 14, we can prove that a bipartite cactus containing no graph in $\mathcal{F}_1$ can be decomposed into graphs which form Fig. 12(b), Fig. 15(a), and a cycle of length 6 whose depth sequence is $(0, 1^-, 2^-, 0, 1^-, 2^-)$ or $(0, 1^-, 2^-, 0, 2^-, 1^-)$.

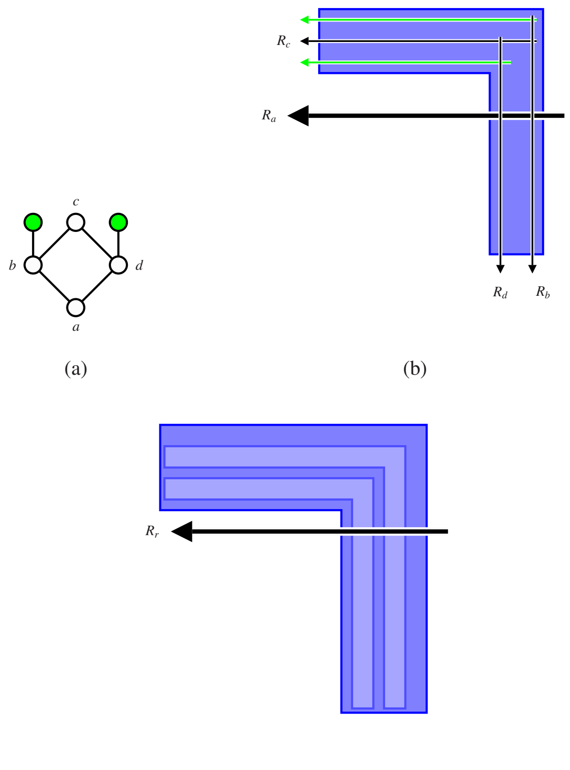

Fig. 13 Diamond and ray representation.

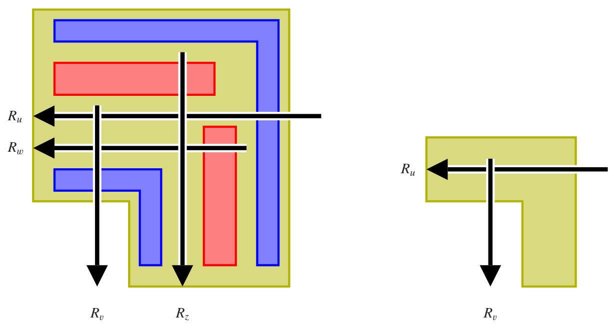

Fig. 14 Ray representation of a graph shown in Fig. 12(b).

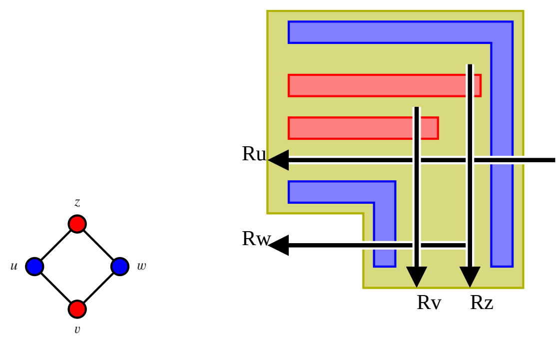

Fig. 15 Diamond with 2 blue vertices and its ray representation.

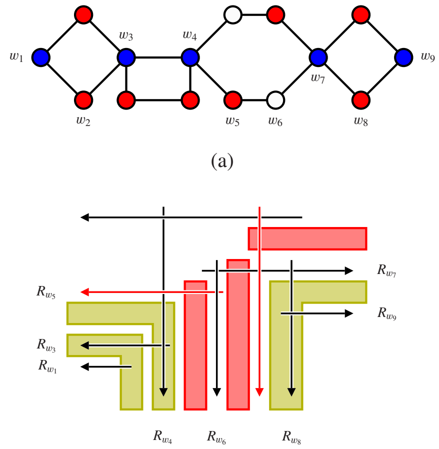

Fig. 16 Example of a cactus and its ray representation

An example of such graph G is shown in Fig. 16(a), where $\langle w_1, w_2, \ldots, w_9\rangle$ is an edge-spine of G. Applying Propositions=4 and 5 along the edge-spine, we can obtain a ray representation shown in Fig. 16(b).

Thus, we have the lemma. ■

4. Proof Sketch of Theorem 3

The following can be done in polynomial time.

- enumerate all cycles in a cactus.
- compute depth sequences of cycles in a cactus.
- compute whether a cactus contain 3-claw.

Therefore, we can compute whether a bipartite cactus contain a graph in $C_{2\times4} \cup \mathcal{F}_2 \cup \mathcal{F}_3$ as an induced subgraph.

Thus from Theorem 2, we have Theorem 3.

References

[1] A.A. Al-Yamani, S. Ramsundar, and D.K. Pradhan, "A defect toler-ance scheme for nanotechnology circuits," IEEE Tranesaction on Circuits and Systems, vol.26, no.1, pp.68–77, 2009.

[2] I. Mustaţă, K. Nishikawa, S. Tayu, and S. Ueno, "On orthogonal ray graphs," Discete Applied Mathematics, vol.158, no.15, pp.1650–1659, 2010.

[3] C.G. Plaxton, "Vertex-weighted matching in two-directional orthogonal," Proc. 24th Internatinoal Symposium on Algorithgms and Computation (ISAAC), Lecture Notes in Computer Science, vol.8283, pp.524–534, 2013.

[4] W. Rao, A. Orailoglu, and R. Karri, "Logic mapping in crossbar-basednanoarchitectures," IEEE Design and Test of Computers, vol.26, no.1, pp.68–77, 2009.

[5] A.M.S. Shrestha, A. Takaoka, S. Tayu, and S. Ueno, "On two problems of nano-pla design," IEICE TRANSACTIONS on Information and Systems, vol.E94-D, no.1, pp.35–41, 2011.

[6] A.M.S. Shrestha, S. Tayu, and S. Ueno, "On orthogonal ray graphs," Discete Applied Mathematics, vol.158, no.15, pp.1650–1659, 2010.

[7] A.M.S. Shrestha, S. Tayu, and S. Ueno, "Bandwidth of convex bipartite graphs and related graphs," Information Processing Letters, vol.112, no.11, pp.411–417, 2012.

[8] M.B. Tahoori, "A mapping algorithm for defect-tolerance of reconfigurable nano-architectures," ICCAD '05: Proc. 2005 IEEE/ACM International Conference on Computer-Aided Desig, pp.668–672, 2005.

[9] A. Takaoka, S. Tayu, and S. Ueno, "Dominatinog sets in two-directional orthogonal ray graphs," IEICE TRANSACTIONS on Information and Systems, vol.E98-D, no.8, pp.1592–1595, 2015.